Investigating the Diameter-Dependent Stability of Single-Walled Carbon Nanotubes

7 AUTHORS, INCLUDING:

Franziska Schaeffel
Schott AG
50 PUBLICATIONS   **771** CITATIONS

SEE PROFILE

Mark H Rümmeli
Leibniz Institute for Solid State and Materi…
172 PUBLICATIONS   **2,546** CITATIONS

SEE PROFILE

Bernd Büchner
Leibniz Institute for Solid State and Materi…
1,042 PUBLICATIONS   **15,116** CITATIONS

SEE PROFILE

George Andrew D Briggs
University of Oxford
472 PUBLICATIONS   **11,743** CITATIONS

SEE PROFILE

Investigating the Diameter-Dependent Stability of Single-Walled Carbon Nanotubes

Jamie H. Warner,[†,]* Franziska Schäffel,[‡] Guofang Zhong,[§] Mark H. Rümmeli,[‡] Bernd Büchner,[‡] John Robertson,[§] and G. Andrew D. Briggs[†]

[†]Department of Materials, University of Oxford, Parks Road, Oxford, OX1 3PH, United Kingdom, [‡]IFW Dresden, P.O. Box 270116, D-01171 Dresden, Germany, and [§]Department of Engineering, The University of Cambridge, 9 JJ Thomson Avenue, Cambridge, CB3 0FA, United Kingdom

ABSTRACT We investigate the long-standing question of whether electrons accelerated at 80 kV are below the knock-on damage threshold for single-walled carbon nanotubes (SWNTs). Aberration-corrected high-resolution transmission electron microscopy is used to directly image the atomic structure of the SWNTs and provides *in situ* monitoring of the structural modification induced by electron beam irradiation at 80 kV. We find that SWNTs with small diameters of 1 nm are damaged by the electron beam, and defects are produced in the side walls that can lead to their destruction. SWNTs with diameters of 1.3 nm and larger are more stable against degradation, and stability increases with diameter. The effect of diameter, defects, and exterior contamination on the inherent stability of SWNTs under electron beam irradiation is investigated.

KEYWORDS: single-walled carbon nanotubes · SWNTs · transmission electron microscopy · HRTEM · electron beam irradiation

Determining the chirality and presence of defects in individual carbon nanotubes is important for correlating structural information with optical, electrical, and magnetic properties. One of the best ways to obtain detailed structural information about individual nanotubes is by using high-resolution transmission electron microscopy (HRTEM) with resolution sufficient to image the carbon atomic structure.[1,2] The small atomic mass of carbon makes it highly susceptible to damage by the electron beam when examined using HRTEM.[3,4] Knock-on structural damage can be significantly reduced by lowering the accelerating voltage of electrons in HRTEM. The advancement of aberration-corrected HRTEM now permits angstrom resolution at a low accelerating voltage of 80 kV and enables the carbon atoms in the sp[2] graphitic nanomaterials such as graphene and SWNTs to be directly imaged.[5,6] While low-voltage HRTEM (LV-HRTEM) has demonstrated its immense power as a technique for determining the chirality of SWNTs[6,7] and the cage structure of single fullerene isomers,[8] the interaction of electrons accelerated at these low voltages with sp[2]-bonded carbon atoms is relatively unknown. The exact value of the knock-on damage threshold is yet to be experimentally determined for SWNTs and fullerenes. It has long been thought that electrons accelerated at 80 kV do not have sufficient energy to induce knock-on damage in SWNTs. We recently showed that fullerenes coalesce inside SWNT peapods under low intensity 80 kV electron beam irradiation without damaging the 1.5 nm SWNT host.[9] Further experiments are needed to develop an understanding of how damage is induced in SWNTs by elec-

trons with sufficiently high intensity for atomic resolution imaging of carbon and what structural transformations occur. This is important for the continual progression and advancement of HRTEM as a technique for analyzing the atomic structure of graphene-based carbon nanomaterials. We directly address the issue of knock-on damage in SWNTs by examining SWNTs with different diameters, cleanliness, and structural integrity.

Several theoretical approaches have been taken to ascertain the electron knock-on cross section of carbon nanotubes and their stability and modification under electron beam irradiation.[10−16] The minimum energy required to be transferred to an individual carbon atom to induce a single monovacancy in the SWNTs has been investigated.[10,12,14,15] Smith *et al.* calculated that a minimum incident electron energy of 86 keV was sufficient to knock carbon atoms from their position within the top and bottom walls, perpendicular to the direction of electron beam propagation.[11] This work was correlated with TEM analysis showing that the damage to SWNTs with prolonged electron beam irradiation at 80 kV was
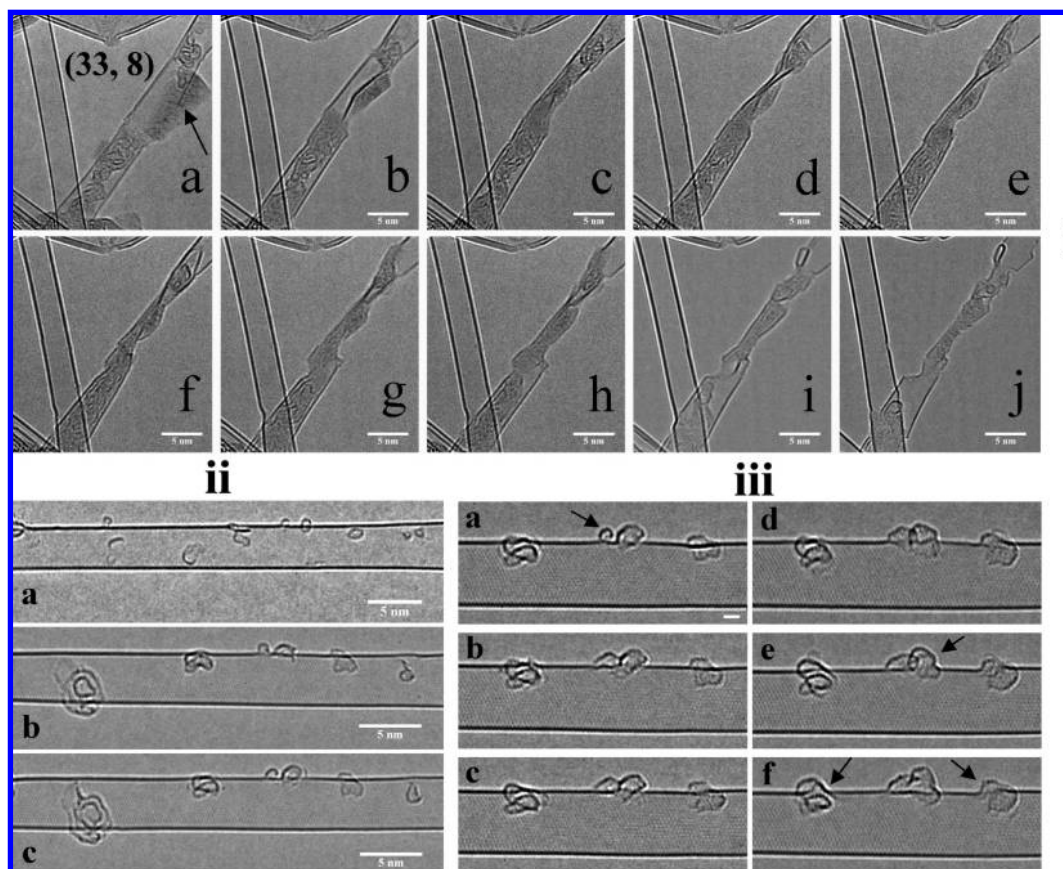
Figure 1. (i) Time series of TEM images showing the rapid destruction of a SWNT contaminated with a large amount of material relative to a clean SWNT with (33,8) chirality. Time between each frame is 5 s. Scale bar indicates 5 nm. (ii) Time series of HRTEM images showing trace amounts of nanocarbon material on the outside. (iii) Time series of HRTEM with higher magnification showing trace amounts of nanocarbon material on the outside. Scale bar indicates 1 nm.

significantly less than at 100 kV.[11] Krasheninnikov *et al.* have investigated the role diameter and chirality of SWNTs plays on their stability under electron irradiation.[15] They determined that the displacement energy for carbon atoms in SWNTs increased as the diameter increased.[15] This means that larger diameter SWNTs should be more robust against electron beam irradiation than smaller ones. Eventually, the displacement energy for very large diameter SWNTs should approach close to that of graphene. Experimental studies on MWNTs under electron beam irradiation have shown the preferential destruction of the inner shell first, due to a higher rate of defect formation.[17] This was related to a lowering of the displacement threshold for the inner nanotube with the highest degree of curvature in its atomic structure.[17] However, a detailed study examining the diameter dependence of SWNT stability under 80 kV electron beam is currently lacking.

The stability of SWNTs under electron beam irradiation is also influenced by the presence of defects, either intrinsic (*i.e.*, formed during the production process) or induced by knock-on displacement from electron beam irradiation. The displacement threshold for carbon atoms situated next to a vacancy is reduced,[10,15] and this can lead to an increase in the sputtering of carbon at-

oms under electron beam irradiation. Thus the presence of vacancies and defects in SWNTs decreases their stability under electron beam damage. Experimental confirmation of this in SWNTs has yet to be fully elucidated using low-voltage atomic-resolution HRTEM. HRTEM examination of SWNTs often requires high electron beam current densities, and theoretical modeling of the resulting structural transformations needs to take into account more than just the initial vacancy formation.[13]

Here, we use aberration-corrected LV-HRTEM with angstrom spatial resolution to directly image the atomic structure of the SWNTs and perform *in situ* measurements regarding the role diameter, defects, and contamination has on the stability of SWNTs using electrons accelerated at 80 kV. Electrons accelerated at 80 kV are supposed to be below the knock-on displacement threshold of SWNTs, and we investigate whether damage is induced in the SWNTs. Time series of HRTEM images are taken to provide *in situ* real-time tracking of the structural modifications. The SWNTs were prepared according to a previously reported procedure.[18] Briefly, the nanotubes were grown as a mat by chemical vapor deposition with a remote microwave plasma from Fe catalyst on Al_2O_3 support layers from hydrogen-

diluted methane at 20 mbar pressure at about 650 °C.[18] SWNTs with exterior contamination required an Fe colloidal catalyst. TEM samples were prepared by first removing the SWNTs from the silicon substrates using a clean razor blade and then dropped into a glass vial. Methanol was then added to the vial, and sonication was applied for 10 min to debundle the originally dense mats of SWNTs. A lacey carbon-coated TEM grid was dipped into the SWNT/methanol solution and allowed to dry. HRTEM was performed using a FEI Titan[3] operating at 80 kV with spherical aberration correction. Electron beam current densities were approximately between 0.1 and 3.0 pA/nm^2. The chirality of the SWNTs was determined by analyzing the 2D fast Fourier transforms to measure the chiral angle vector. Line profiles measuring the gray scale intensity across the axis of the SWNT were taken to determine the diameter. Knowledge of the chiral angle vector combined with the diameter and tilt enables the SWNT chirality to be evaluated.

Figure 2. Time series of HRTEM images showing the rapid destruction of a (7,7) SWNT with defects compared to the defect-free (9,6) SWNT.

During our investigation, we made sure that we compared SWNTs that received identical dosages of electrons. This was achieved by finding areas containing multiple SWNTs of interest in close proximity. This also ensured that the contact of the SWNTs with the TEM grid was similar, and effects such as heating and the dissipation of heat would be the same during the exposure period. We found that SWNTs that were contaminated with material deposited on the surface were unstable under constant electron beam irradiation. The material on the outside of the SWNT consisted of amorphous carbon and possibly residue Fe from the catalyst used in the growth procedure. We observed crystalline lattice fringes in parts of the contamination with lattice spacing of 0.34 nm. Figure 1i shows a time series of HRTEM images of two SWNTs under constant electron beam irradiation, with 5 s between each image. Figure 1ia shows a pristine 3 nm diameter SWNT with chirality indexed to (33,8) on the left and a 3.2 nm diam-
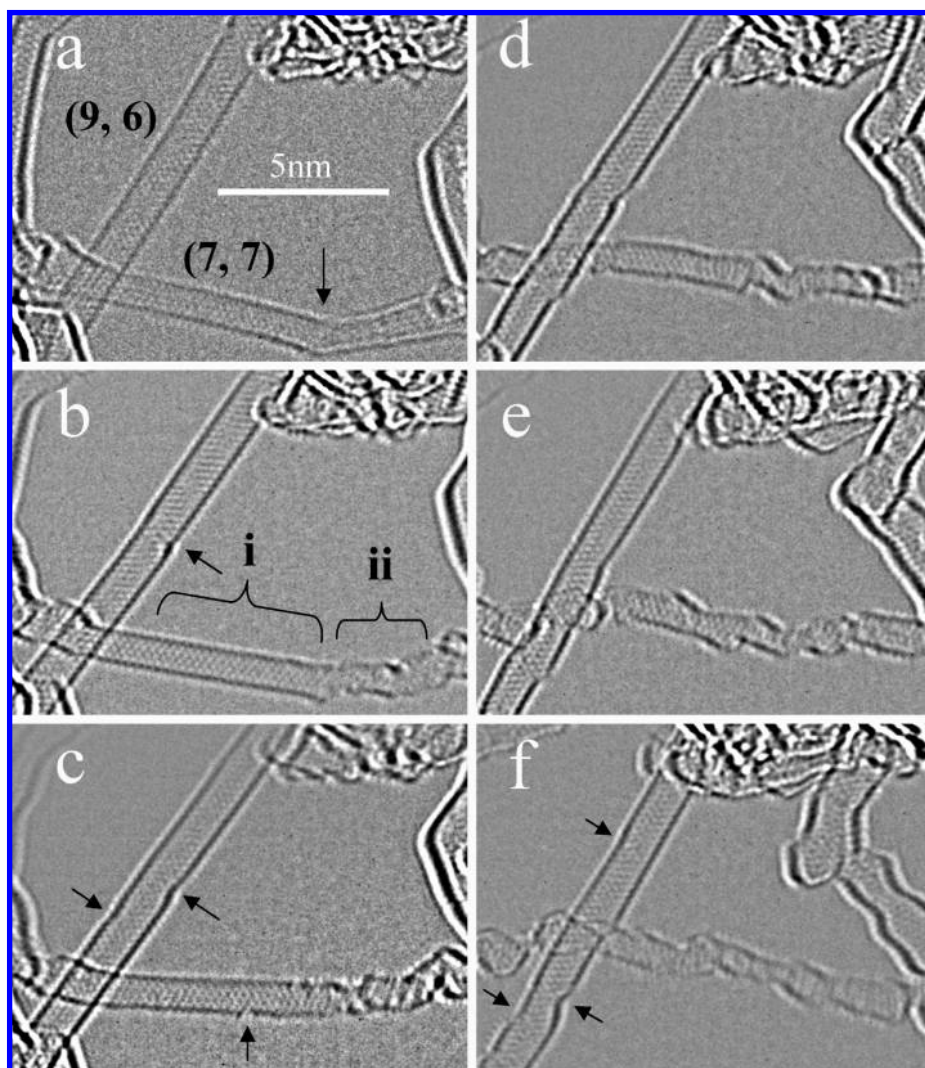
eter SWNT contaminated with material on the outside on the right, indicated with an arrow (see Supporting Information). The presence of material on the outside of the SWNT results in rapid deformation of the SWNT when exposed to electron beam irradiation, even at the low accelerating voltage of 80 kV. Figure 1ib shows that after only 5 s significant distortion occurs. As time goes on for a further 40 s (Figure 1ic−j), the SWNT contaminated with material is destroyed, while the pristine (33,8) SWNT to the left remains relatively unchanged. It is important to note that both the pristine and dirty SWNT are in close proximity and thus receive almost identical electron beam dosage and are contacted to the copper grid and rest of the sample in a similar manner. This enables a direct comparison of electron beam induced effects over the time period shown in Figure 1i. These results demonstrate that the stability of SWNTs is significantly increased if the outer surface is pristine. We attribute this reduced stability to the material on the outside the SWNT reacting with the SWNT to disrupt the sp^2 carbon bonding and the
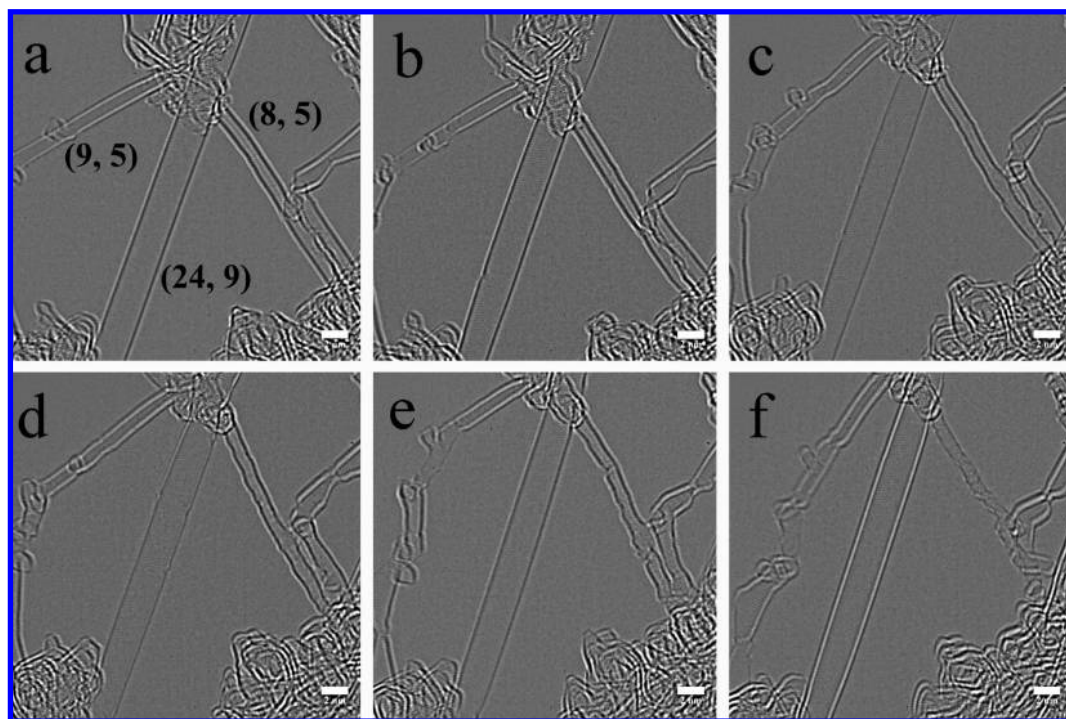
Figure 3. Time series of HRTEM images showing the SWNTs with smaller diameter ((8,5) and (9,5)) and are destroyed faster than the larger diameter SWNT (24,9). Scale bar indicates 2 nm.

subsequent structural rearrangement of the SWNT leading to shape deformation. The amorphous carbon on the outside of the SWNT contains many dangling bonds that are chemically reactive. The possible presence of Fe atoms would also lead to reactions with the surrounding carbon. Energy provided by the electron beam may be sufficient to instigate reactions with neighboring carbon atoms on the SWNT and change their bonding and lead to distortion of the SWNT graphitic lattice structure. Damage to the sp^2 bonding structure in the SWNT and the presence of unsaturated carbon atoms will increase the susceptibility for electron beam induced sputtering. In Figure 1i, we see both the removal of a large amount of carbon *via* electron beam induced sputtering, along with the SWNT undergoing structural rearrangement to compensate. Yuzvinsky *et al.* have shown that the addition of contaminants such as oxygen and water reduces the damage threshold of MWNTs and enables precision cutting of the MWNT at a low electron accelerating voltage of 1 kV.[19] Without the contaminants reacting with the surface of the MWNTs, they remained stable under electron beam irradiation at 1 kV.[19]

We found that small nanometer-sized carbons present on the outer surface of the larger diameter SWNTs were initially mobile under electron beam irradiation. However, after a few minutes of electron beam irradiation, the trace amounts of nanocarbon material were incorporated into the side-wall structure of the SWNT. The incorporation of these trace amounts of carbon into the SWNT structure resulted in only localized structural changes that were not significant enough to

induce large-scale shape rearrangement that was observed in Figure 1i. Figure 1iia shows a section of a SWNT containing approximately 10 nanocarbon pieces on the surface. Figure 1iib shows a higher magnification of this same SWNT after 20 s of electron beam irradiation. Several of the small nanocarbon pieces have changed shape and position. This is continued for another 20 s, as shown in Figure 1iic. In Figure 1iii, we increased the magnification in the HRTEM in order to examine how the nanocarbon pieces interact with the outer surface of the SWNT and the structural changes that result. The time between images is 20 s. During the irradiation process (Figure 1iiia−f), the size of the nanocarbon material increased, especially the two pieces indicated with an arrow in Figure 1iiia. The increase in size requires additional carbon material, which must come from either the SWNT or the diffusion of carbon atoms along the surface of the SWNT from a larger feedstock area on the TEM grid. In Figure 1iiie, the side wall of the SWNT has been opened to form a small bubble on the surface, indicated with an arrow. This is also seen in the two other sections in Figure 1iiif, and surprisingly, the opening of the side wall observed in the middle section in Figure 1iiie is now closed with the outer bubble remaining. Overall, we found that the larger 3 nm SWNTs remained structurally stable when the amount of contamination on the outer SWNT was present in only trace amounts and consisted of only carbon and not catalytic metals such as Fe.

Next we examined how the presence of defects affected the stability of clean SWNTs. Figure 2a shows a HRTEM image of two SWNTs. The 1 nm diameter SWNT

on the left is nearly defect-free with (9,6) chirality, and the 0.9 nm diameter SWNT below has (7,7) chirality and contains a large defect, indicated with an arrow. Figure 2a−f is a time series of HR-TEM images showing the effect a defect has on the stability of SWNTs under constant electron beam irradiation. The time between each frame is 20 s. Figure 2b shows that after only 20 s region (ii) of the (7,7) SWNT has been significantly damaged compared to region (i) and the (9,6) SWNT. Twenty seconds later, in Figure 2c, the defective region (ii) has merged with the pristine region (i) and the entire SWNT has straightened out. We observed that electron beam irradiation at 80 kV created new defects in the pristine side walls of a SWNT; these new defects are indicated with arrows in Figure 2b−d. Figure 2f shows that after 100 s of electron beam irra-
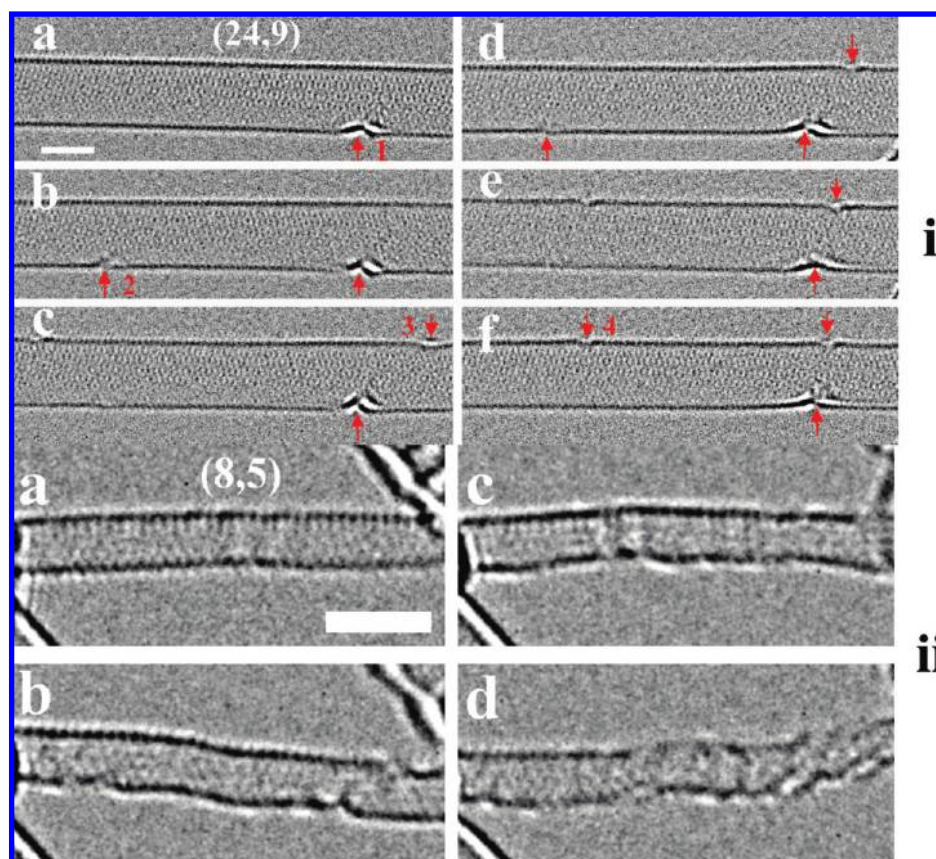

Figure 4. (i) Time series of HRTEM images of a large 2.3 nm diameter (24,9) SWNT under constant electron beam irradiation. Arrows indicate the presence of defects. Time between frames is 5 s. Scale bar indicates 2 nm. (ii) Time series of HRTEM images of a narrow 0.89 nm diameter (8,5) chirality SWNT under constant electron beam irradiation. Time between frames is 20 s. Scale bar indicates 2 nm.

diation the defective (7,7) SWNT is largely distorted with significant damage as compared to the (9,6) SWNT. The (9,6) SWNT remains intact with only a few defects induced into the side walls of the SWNT. This series of HRTEM images reveals that SWNTs with defects are less stable under electron beam irradiation than high-quality defect-free SWNTs. Carbon atoms situated around a defect in SWNTs are often unstable and reactive. These results agree with the theoretical work of Crespi *et al.*[9] and Krasheninnikov *et al.*[16] that predicts defective SWNTs are less stable than defect-free SWNTs. Figure 2 shows that electron beam irradiation at an accelerating voltage of 80 kV does result in the formation of new defects in narrow 1 nm diameter SWNTs in regions that were originally pristine.

We observed that SWNTs with small diameters seemed to degrade faster than their larger diameter counterparts. In order to examine this, we located a region of the sample that contained both large (~2−3 nm) and small (~1 nm) diameter SWNTs next to each other. This enables the same electron beam dosage to be applied to both narrow and large diameter SWNTs and provides a true comparison of diameter-dependent effects. Figure 3a shows a HRTEM image of a region containing three SWNTs, one large 2.3 nm diameter SWNT with (24,9) chirality and two smaller SWNTs with

(9,5) and (8,5) chiralities and diameters of 0.96 and 0.89 nm, respectively. Figure 3a−f shows a time series of HRTEM images with 20 s between each image. Figure 3f shows that after 100 s of constant electron beam irradiation the two smaller SWNTs have undergone significant structural deformation, while the larger (24,9) SWNT remains relatively unchanged.

The effect of electron beam irradiation on the SWNT atomic structure is shown in more detail in Figure 4i,ii. Figure 4ia−f shows a time series of HRTEM images of the 2.3 nm diameter (24,9) chirality SWNT after an initial 60 s of electron beam irradiation. The time between each frame is 5 s. Arrows are included to indicate the presence of a defect in the side wall of the SWNT. In Figure 4ia, a defect (1) is present in the bottom section of the SWNT, while the rest of the SWNT remains pristine. Figure 4ib shows that 5 s later a new defect (2) appears to the left. In Figure 4ic, another new defect (3) appears in the top right-hand side of the SWNT. As time progresses (Figure 4ic−f), defect (3) in the top region moves along the nanotube to the left-hand side to become almost vertically aligned with the large defect (1) in the bottom side of the SWNT. A new smaller defect (4) also emerges in the top side to the left of the SWNT. Figure 4if also shows that defect (2) is no longer present and was only temporarily observable. This may be due
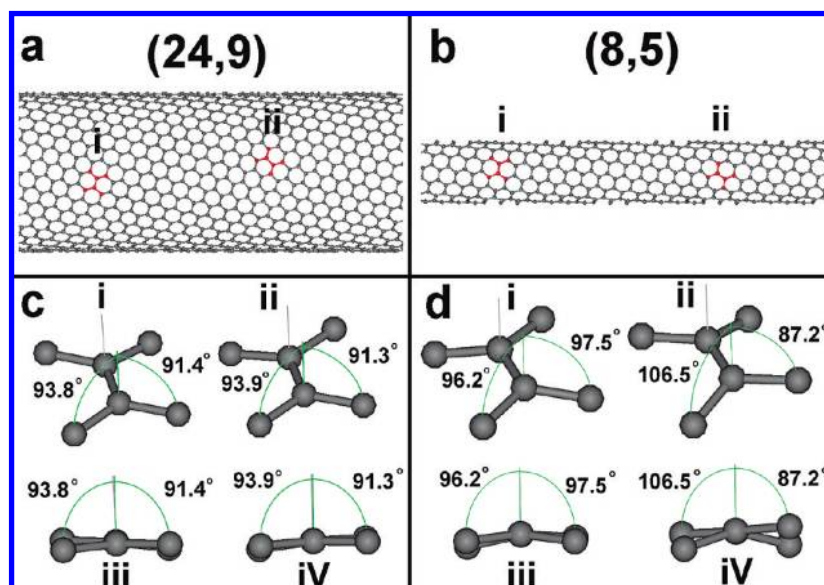
Figure 5. Structural model with the back half removed showing the atomic structure of (a) (24,9) and (b) (8,5) SWNTs. Two sets of carbon atom directions with different strain are indicated with (i) and (ii) and highlighted in red. (c)(i) Three-dimensional view of the carbon atoms indicated in (a)(i) with measurement of the angles used for determining the pyramidalization angle. (ii) Three-dimensional view of the (24,9) SWNT carbon atoms indicated in (a)(ii) with measurement of the angles used for determining the pyramidalization angle. (iii) End-on view of (c)(i). (iv) End-on view of (c)(ii). (d)(i) Three-dimensional view of the (8,5) SWNT carbon atoms indicated in (b)(i) with measurement of the angles used for determining the pyramidalization angle. (ii) Three-dimensional view of the carbon atoms indicated in (b)(ii) with measurement of the angles used for determining the pyramidalization angle. (iii) End-on view of (d)(i). (iv) End-on view of (d)(ii).

the higher the strain in the carbon bonds. Higher strain in the chemical bonds results in reduced stability and increased reactivity.[20] We used the CoNTub algorithm[21] to generate structural models of (24,9) and (8,5) SWNTs in order to investigate the diameter-dependent strain on the carbon bonds. Figure 5a shows the atomic structure of one wall of the (24,9) SWNT. The back wall has been removed for clarity of presentation and ease of analysis. Strain is induced differently to carbon atoms depending upon their direction with respect to the axis of the SWNT. There exist two sets of carbon atoms with similar strain profiles, and these are illustrated in Figure 5a,b, by labeling with (i) and (ii) and in red color. Higher strain is induced upon the set of carbon atoms labeled (ii) due to their direction with respect to the curvature of the SWNT. Figure 5c,d analyzes the strain in each of these systems. Figure 5ci shows a 3D view of the set of carbon atoms in Figure 5ai, and Figure 5cii shows a 3D view of the set of carbon atoms in Figure 5aii. We measured two angles for each set of carbon atoms that can be used to determine the pyramidalization angle, θ_p.[20] The pyramidalization angle can be determined by summing these two angles together, then subtracting 180° and then dividing by 2. This gives $\theta_p(i) = 2.6°$ for the set of carbon atoms (i) for a (24,9) SWNT. We find $\theta_p(ii) = 2.6°$ for the set of carbon atoms (ii) for a (24,9) SWNT. Figure 5ciii,iv shows the end-on view of the set of carbon atoms presented above in Figure 5ci,ii, respectively. Similar measurements were taken on the (8,5) SWNT and are shown in Figure 5d. We find $\theta_p(i) = 6.85°$ and $\theta_p(ii) = 6.85°$ for the (8,5) SWNT. While the pyramidalization angle is the same for both sets of carbon atoms in both the (24,9) and (8,5), there is a major difference in the misalignment of the π orbitals, which is suggested as the main source of strain in carbon nanotubes.[20] The misalignment of π orbitals can be seen when examining the end-on view presented in Figure 5ciii,iv and diii,iv. When there is no misalignment, the end-on view should give the appearance of only three carbon atoms. Misalignment results in an angle between the back three carbon atoms and the front three and the appearance of five carbon atoms. The largest misalignment of the π orbitals is seen in Figure 5div. We measured π orbital misalignment angles, φ, for (24,9) SWNT as $φ(i) = 7.0°$ and $φ(ii) = 3.5°$, and for (8,5) SWNTs as $φ(i) = 4.7°$ and $φ(ii) = 17.5°$. This reveals a significantly larger strain is present in the (8,5) SWNT as compared to the (24,9) SWNT due to the larger π orbital misalignment. The re-

to the SWNT heating up from the electron beam irradiation and the subsequent effects of annealing. This shows that defects are induced in the side walls of the SWNTs and they are mobile and in some circumstances only temporary. Figure 4ii shows a time series of HRTEM images of the narrow 0.89 nm diameter (8,5) chirality SWNT. The time between each frame is 20 s. Figure 4iia shows the (8,5) SWNT at the beginning of the electron beam irradiation with pristine structure. Figure 4iid shows that after 60 s of electron beam irradiation the atomic structure of the SWNT is extremely distorted and no longer represents a (8,5) SWNT. The mechanism behind the time-dependent evolution of damage that we observe in HRTEM involves several competing effects such as electron beam induced thermal annealing that can heal defects and electrostatic charging. Electron beam irradiation can induce electronic excitations that lead to weakening of the carbon bonds, and this may lead to a reduction in the energy required for atomic displacement.

The HRTEM results from Figures 3 and 4i,ii demonstrate that larger diameter SWNTs are more stable under electron beam irradiation than smaller diameter SWNTs, in agreement with the theoretical work of Krasheninnikov *et al.*[15] When a sheet of graphene is rolled up to form a SWNT, strain is induced on the carbon bonds due to the curvature of the SWNT.[20] The narrower the diameter of the SWNT, the tighter the graphene sheet has to be rolled to form a SWNT and

sults presented in Figures 3 and 4 show a direct correlation between the strain induced upon the carbon bonds by the curvature of SWNTs and their stability we observed under electron beam irradiation.

In summary, we have examined how electrons accelerated at 80 kV interact with SWNTs. We showed that SWNTs contaminated with large amounts of dirt/material on the outside were unstable. When only trace amounts of nanocarbon was present on the surface of larger 3 nm diameter SWNTs, it was incorporated into the side walls of the SWNTs after prolonged electron beam irradiation. SWNTs with significant defects were unstable and degraded faster than pristine SWNTs. We showed that the stability of SWNTs increases with increasing diameter. These results correlate well with the theoretical calculations involving SWNTs under electron beam irradiation.[10−16] SWNTs with subnanometer diameters were very prone to electron beam induced structural damage. In larger 2−3 nm diameter SWNTs, defects were mobile and in some cases only lasted temporarily. Most importantly, although it has long been thought that 80 kV might be below the knock-on damage threshold for SWNTs, we find electron beam irradiation still produces defects in pristine SWNTs resulting in damage. However, the beam current densities we used were large and excessive, and by lowering this, damage may be avoided for sufficiently long periods of time. These results indicate that extreme care must be taken when performing *in situ* HRTEM chirality determination of SWNTs in applications such as FET devices where damage to the structure is unwanted.

Supporting Information Available: HRTEM image processing, chirality determination, HRTEM images of crystalline contamination on outside of SWNTs. This material is available free of charge *via* the Internet at http://pubs.acs.org.

REFERENCES AND NOTES

1. Hashimoto, A.; Suenaga, K.; Gloter, A.; Urita, K.; Iijima, S. Direct Evidence for Atomic Defects in Graphene Layers. *Nature* **2004**, *430*, 870–873.
2. Suenaga, K.; Wakabayashi, H.; Koshino, M.; Sato, Y.; Urita, K.; Iijima, S. Imaging Active Topological Defects in Carbon Nanotubes. *Nature* **2007**, *2*, 358–360.
3. Egerton, R. F.; Li, P.; Malac, M. Radiation Damage in the TEM and SEM. *Micron* **2004**, *35*, 399–409.
4. Krasheninnikov, A. V.; Banhart, F. Engineering of Nanostructure Carbon Materials with Electron or Ion Beams. *Nat. Mater.* **2007**, *6*, 723–733.
5. Warner, J. H.; Ruemmeli, M. H.; Gemming, T.; Buechner, B.; Briggs, G. A. D. Direct Imaging of Rotational Stacking Faults in Few Layer Graphene. *Nano Lett.* **2009**, *9*, 102–106.
6. Sato, Y.; Yanagi, K.; Miyata, Y.; Suenaga, K.; Kataura, H.; Iijima, S. Chiral-Angle Distribution for Separated Single-Walled Carbon Nanotubes. *Nano Lett.* **2008**, *8*, 3151–3154.
7. Guan, L.; Suenaga, K.; Iijima, S. Smallest Carbon Nanotube Assigned with Atomic Resolution Accuracy. *Nano Lett.* **2008**, *8*, 459–462.
8. Sato, Y.; Suenaga, K.; Okubo, S.; Okazaki, T.; Iijima, S. Structures of $D_{5d}−C_{80}$ and $I_h−Er_3N@C_{80}$ Fullerenes and Their Rotation Inside Carbon Nanotubes Demonstrated by Aberration-Corrected Electron Microscopy. *Nano Lett.* **2007**, *7*, 3704–3708.
9. Warner, J. H.; Ito, Y.; Zaka, M.; Ge, L.; Akachi, T.; Okimoto, H.; Porfyrakis, K.; Watt, A. A. R.; Shinohara, H.; Briggs, G. A. D. Rotating Fullerene Chains in Carbon Nanopeapods. *Nano Lett.* **2008**, *8*, 2328–2335.
10. Crespi, V. H.; Chopra, N. G.; Cohen, M. L.; Zettl, A.; Louie, S. G. Anisotropic Electron-Beam Damage and the Collapse of Carbon Nanotubes. *Phys. Rev. B.* **1996**, *54*, 5927–5931.
11. Smith, B. W.; Luzzi, D. E. Electron Irradiation Effects in Single Wall Carbon Nanotubes. *J. Appl. Phys.* **2001**, *90*, 3509–3515.
12. Zobelli, A.; Gloter, A.; Ewels, C. P.; Siefert, G.; Colliex, C. Electron Knock-on Cross Section of Carbon and Boron Nitride Nanotubes. *Phys. Rev. B* **2007**, *75*, 245402.
13. Yasuda, M.; Kimoto, Y.; Tada, K.; Mori, H.; Akita, S.; Nakayama, Y.; Hirai, Y. Molecular Dynamics Study of Electron-Irradiation Effects in Single-Walled Carbon Nanotubes. *Phys. Rev. B* **2007**, *75*, 205406.
14. Lu, A. J.; Pan, B. C. Nature of Single Vacancy in Achiral Carbon Nanotubes. *Phys. Rev. Lett.* **2004**, *92*, 105504.
15. Krasheninnikov, A. V.; Banhart, F.; Li, J. X.; Foster, A. S.; Nieminen, R. M. Stability of Carbon Nanotubes under Electron Irradiation: Role of Tube Diameter and Chirality. *Phys. Rev. B* **2005**, *72*, 125428.
16. Ajayan, P. M.; Ravikumar, V.; Charlier, J.-C. Surface Reconstructions and Dimensional Changes in Single-Walled Carbon Nanotubes. *Phys. Rev. Lett.* **1998**, *81*, 1437–1440.
17. Banhart, F.; Li, J. X.; Krasheninnikov, A. V. Carbon Nanotubes under Electron Irradiation: Stability of the Tubes and Their Action as Pipes for Atom Transport. *Phys. Rev. B* **2005**, *71*, 241408(R) .
18. Zhong, G.; Iwasaki, T.; Robertson, J.; Kawarada, H. Growth Kinetics of 0.5 cm Vertically Aligned Single-Walled Carbon Nanotubes. *J. Phys. Chem. B* **2007**, *111*, 1907–1910.
19. Yuzvinsky, T. D.; Fennimore, A. M.; Mickelson, W.; Esquivias, C.; Zettl, A. Precision Cutting of Nanotubes with Low-Energy Electron Beam. *Appl. Phys. Lett.* **2005**, *86*, 053109.
20. Niyogi, S.; Hamon, M. A.; Hu, H.; Zhao, B.; Bhowmik, P.; Sen, R.; Itkis, M. E.; Haddon, R. C. Chemistry of Single-Walled Carbon Nanotubes. *Acc. Chem. Res.* **2002**, *35*, 1105–1113.
21. Melchor, S.; Dobado, J. A. CoNTub: An Algorithm for Connecting Two Arbitrary Carbon Nanotubes. *J. Chem. Inf. Comput. Sci.* **2004**, *44*, 1639–1646.